INTERNATIONAL JOURNAL OF AUTOMOTIVE AND MECHANICAL ENGINEERING
ISSN: 2229-8649 e-ISSN: 2180-1606
VOL. 21, ISSUE 3, 2024, 11581 – 11595
DOI: https://doi.org/10.15282/ijame.21.3.2024.10.0893

RESEARCH ARTICLE

Wheel Slip Equilibrium Point Model Reference Adaptive Control Based PID Controller for Antilock Braking System: A New Approach

P. C. Eze[1,2*], D. O. Njoku[3], O. C. Nwokonkwo[4], C. G. Onukwugha[3], J. N. Odii[3] and J. E. Jibiri[4]

[1]Department of Electrical and Electronic Engineering, Imo State University, Owerri, Nigeria
[2]Department of Electrical and Electronic Engineering, Federal University of Technology, Owerri, Nigeria
[3]Department of Computer Science, Federal University of Technology, Owerri, Nigeria
[4]Department of Information Technology, Federal University of Technology, Owerri, Nigeria

ABSTRACT - This paper presents a new approach to wheel slip control in Antilock Braking System (ABS) using an Approximated First Order Wheel Slip (AFOWS) Model Reference Adaptive Control (MRAC) based PID (AFOWS-MRAC-PID) controller. An ABS was modeled in a MATLAB/Simulink environment using a quarter car model with the proposed controller. Simulations were conducted with a wide range of adaptation gains (50, 100, 150, 200, and 250) to study the effectiveness of the proposed control system. The results revealed that the proposed system could track and maintain 10% wheel slip and eliminate oscillation (instability) in terms of overshoot associated with conventional PID controllers, particularly on wet and snowy road surfaces, using adaptation gains of 150, 200, and 250. Overall, the proposed system provided the best performance in terms of stopping distance, vehicle braking velocity, and braking torque on all road surfaces with an adaptation gain of 250, although braking on dry road surfaces was the most effective.

ARTICLE HISTORY
Received : 25th Oct. 2023
Revised : 22nd Mar. 2024
Accepted : 19th Aug. 2024
Published : 20th Sept. 2024

KEYWORDS
Antilock braking system
Controller
MRAC
PID
Wheel slip equilibrium point

1. INTRODUCTION

During normal braking, the Antilock Braking System (ABS) does not control slip. Slip, defined as the difference between vehicle speed and wheel speed, is typically expressed as a percentage. It becomes significant during hard braking, particularly in emergencies or on unfavorable road surfaces. Such conditions can include sand, mud, ice, snow, rocks, and both wet and dry surfaces. Poor road conditions can adversely affect a vehicle's motion—whether accelerating or decelerating—causing it to spin during acceleration or skid when the wheels lock up during deceleration [1]. This underscores the necessity of slip control in ABS to enhance passenger safety and minimize the risk of various vehicle crashes, including run-off incidents. ABS is a crucial component in modern vehicles, ensuring safety during emergency or hard braking by maintaining steerability and stability while preventing wheel lock-up. When the wheels slip and lock up during hard braking, the stopping distance is extended, potentially leading to a loss of steering stability [2,3]. Therefore, ABS is designed with slip control to regulate wheel slip, ensuring optimal traction and maintaining steering stability [4]. The vehicle's wheel slip ratio during hard braking is determined by the tires' ability to maintain optimal grip on the road surface [5], which enables the vehicle to stop within the shortest possible distance while retaining directional control [6].

The slip control law in ABS is generally designed to prevent wheel lock-up and maintain optimal traction between the tires and the road surface during severe braking. Achieving maximum traction is challenging because the relationship between wheel slip and friction varies with vehicle dynamics, tire characteristics, and road conditions [6]. Therefore, the ABS controller must be robust and adaptive to manage any distortions or mismatches in system parameters. The objective of this paper is to present a novel slip control algorithm based on an approximate first-order model of wheel slip around the equilibrium point, aimed at maintaining optimal slip levels during severe braking. The proposed system employs a Model Reference Adaptive Control (MRAC) based Proportional Integral and Derivative (PID) algorithm, providing adaptive and robust control across different road surfaces with a wide range of adaptation gains, which inspired this research. The algorithm is named the Approximate First Order Wheel Slip Model Reference Adaptive Control based PID (AFOWS-MRAC-PID) controller.

The remainder of this paper is structured as follows: Section 2 provides a brief overview of previous studies on slip control in ABS. Section 3 details the methodology used to achieve the study's objectives. Section 4 presents the simulation results from the analysis conducted in the MATLAB/Simulink environment. Finally, Section 5 concludes the study.

2. RELATED WORK

There are various control systems for ABS, all aiming to achieve optimal tracking of the wheel slip ratio during emergency or hard braking. This section provides a brief yet comprehensive review of related works to broaden understanding of recent control approaches applied in ABS. PID controllers have been proposed for wheel slip control in vehicles, with their longitudinal dynamics described using a Five-Degree of Freedom (5-DOF) model and a quarter car

***CORRESPONDING AUTHOR | Paulinus Chinaenye Eze** | ✉ paulinuseze1@gmail.com

model by [1] and [7], respectively. Similarly, [8] used a PID controller to investigate the effect of different aerodynamic drag forces on ABS performance. A hybrid control system, combining Feedback Linearization (FBL) and PID control, was employed to achieve wheel slip control using a quarter-car model [9].

A self-tuning PID controller that uses a fuzzy algorithm for tuning has been applied in ABS with an Electronic Wedge Brake (EWB) based on a 2-DOF dynamic traction (quarter car) model of a vehicle. This approach aimed to improve stopping time, stopping distance, settling time, and target slip compared to a benchmark ABS based on PID control and a fuzzy fractional PID technique [10]. In [11], a Fuzzy Logic Controller (FLC) was proposed as a promising alternative to the classical PID algorithm, achieving three control objectives: reducing stopping distance, limiting slip ratio, and improving control performance. Other techniques based on fuzzy logic algorithms, such as Fuzzy Gradient Control (FGC) in electric vehicles, Adjustable Gain Enhanced Fuzzy Logic Control (AGE-FLC), and Fuzzy Logic Control with Variable Zero Lag Compensator (FLC-VZLC) used in a quarter car model for vehicle braking at a given speed, have been proposed for ABS to reduce stopping distance and improve wheel-slip performance during emergency braking [4,5,12]. An improved optimal slip ratio control was achieved using a Fuzzy-PID controller that accounted for changes in tire pressure [13]. Additionally, wheel slip control in ABS based on adaptive techniques, such as Genetic fuzzy self-tuning PID controllers, neuro-fuzzy systems, and fuzzy genetic algorithms, has been separately implemented to improve slip tracking and stopping distance [14-16]. For vehicle stability control and complex braking maneuvers in ABS and the Electronic Stability Program (ESP), FLC was implemented in a Sport Utility Vehicle (SUV) and examined for braking on different road surfaces [17]. An adaptive controller based on a fuzzy logic control algorithm was used to regulate wheel slip on dry, wet, and icy road surfaces during braking for an SUV [18]. Fuzzy-PID controllers were also used to achieve optimal slip ratios for cornering braking control of a motorcycle [19].

Sliding Mode Control (SMC) and its modified algorithms, such as Grey Sliding Mode Control (GSMC) and Improved Sliding Mode Control (ISMC), have been utilized to achieve faster dynamic response, stability, and robustness in vehicle wheel-slip control systems [20,21]. ABS slip performance has been enhanced by eliminating the chattering effect associated with SMC using Fuzzy Sliding Mode Control (FSMC) [22,23]. Considering both nonlinear and purely linear relationships between friction and slip, a Higher-order Sliding Mode Observer (HSMO) and a first-order Sliding Mode Observer (SMO) were separately designed for ABS control [24]. ABS control was also developed based on the dynamic analysis of hydraulic braking systems using integrated Nonlinear Tracking Control (NTC), a nonlinear observer, to achieve wheel slip control [25]. Two adaptive nonlinear control systems based on the Time Varying Asymmetric Barrier Lyapunov Function (TABLF) were employed in ABS to achieve optimal wheel slip ratio tracking using a quarter car model [26]. The issue of self-locking in the wheels of aircraft landing systems using ABS, considering the braking operating status region, was addressed with an Asymmetric Barrier Lyapunov Function (ABLF)-based wheel slip controller. This system eliminated self-locking and provided zero steady-state error in tracking the optimal wheel slip ratio [27].

The reviewed related works indicate that promising results have been achieved in previous studies regarding wheel slip minimization in ABS. However, most prior works did not assess the effectiveness of control techniques concerning changes in road conditions or consider essential vehicle dynamics, such as air drag force and wheel viscous force, which may affect the performance of the wheel slip controller [5]. These gaps are addressed in this paper. Additionally, relying solely on a PID controller can make the system susceptible to parameter mismatch and distortion. Some disadvantages of FLC systems include susceptibility to steady-state error [4], difficulty in accurately determining membership functions, lack of a logical method to transform expert knowledge into rule bases, and time-consuming parameter tuning [28]. The challenges of expert PID and fuzzy-PID controllers include sub-par timing precision and limited anti-interference capabilities [29]. Sliding Mode Control (SMC) is prone to chattering, which results from the nonlinear dynamic equations of the wheel slip control system and can impact the lifespan of components [5]. Therefore, a novel approach is proposed based on using an established first-order equation of wheel slip around the equilibrium point as a reference model to develop an MRAC-based PID controller for ABS. This ensures the system operates at the well-known wheel slip equilibrium point and provides a wide range of adaptability using a simplified control algorithm.

3. SYSTEM DESIGN

3.1 Dynamic Motion Equations of Braking Vehicle

A quarter car model (or single tire model) shown in Figure 1 is used to describe the dynamic motion of a braking vehicle. Hence, the equations representing its dynamic behaviors are presented for a straight-line braking car. The assumptions made regarding the braking car are:

a) The car's deceleration occurs on a straight path and can be described by linear motion equations.

b) The car's movement in vertical and lateral directions is negligible.

c) The car brakes with the speed of 30 ms^{-1} at the initial stage on a straight path.

The dynamic equations of the braking vehicle with respect to Figure 1 are given in terms of frictional force, vehicle forward motion, rotational dynamic of the wheel, actuator dynamic, tire-friction dynamic, and slip equation.

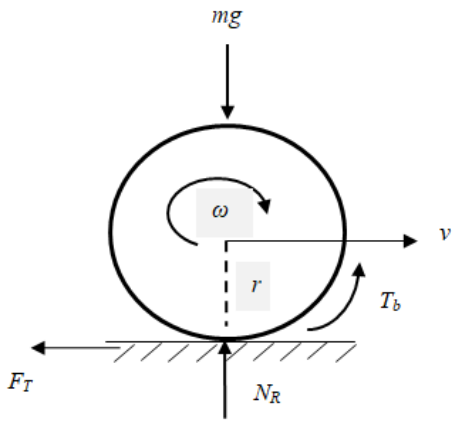

Figure 1. Single tire description

The frictional force equation can be described by:

$$F_T = \mu(\lambda)N_R \tag{1}$$

where $\mu(\lambda)$stands for friction coefficient and depends on wheel slip, N_R reaction force in Newton.

During braking, the linear motion is determined in accordance with Newton's laws of motion and it is expressed in terms of the summation of the forces acting on the vehicle by:

$$\sum F \geq F_T + F_d\,, \qquad \sum F = ma \tag{2}$$

where a is the vehicle's acceleration in ms^{-2}, m stands for the vehicle's mass, and F_d is the vehicle's aerodynamics. Thus, the vehicle's deceleration is given by:

$$a = -\frac{1}{m}\left[\mu(\lambda)N_R + \frac{1}{2}ADCv^2\right] \tag{3}$$

where $\frac{1}{2}ADCv^2$ is the aerodynamic drag force expression with A, C, D, and v representing the projected area of the vehicle, drag coefficient, air density, and braking speed in ms^{-1}. Expressing Equation (3) in terms of braking speed gives:

$$\dot{v} = -\frac{1}{m}\left[\mu(\lambda)N_R + \frac{1}{2}ADCv^2\right] \tag{4}$$

As the vehicle exhibits translational motion while decelerating to a halt, the wheel rotates such that its rotational dynamic is defined by:

$$\dot{\omega} = \frac{1}{J}[r\mu(\lambda)N_R - f_w\omega - T_b(sign(\omega))] \tag{5}$$

where ω is the wheel's angular speed, J stands for the moment of inertia of the vehicle, r represents the radius of the wheel, f_w stands for viscous friction of the wheel and T_b represents braking torque.

A transfer function of the first order dynamic is used to describe the hydraulic brake actuator and is defined in [1,5,30] as:

$$G(s) = \frac{k}{\tau s + 1} \tag{6}$$

where k stands for the braking gain and depends on different quantities such as brake radius, the friction coefficient of the brake pad, the number of pads and brake temperature [31]. Introducing a time delay function $e^{-s\tau}$ into Equation (6) for fluid lag or delay compensation gives [1,5]:

$$T_b = e^{-s\tau}\frac{k}{\tau s + 1}T_{ref}, \quad where\ G(s) = \frac{T_b}{T_{ref}} \tag{7}$$

In this paper, a limit $T_{max} = 4000$ Nm constranied to $0 < T_b < T_{max}$ is considered for the maximum braking torque [32]. Figure 2 is the actuator's model in Simulink.

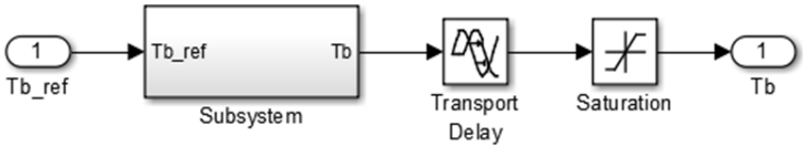

Figure 2. Actuator model in Simulink

For the friction between the tire and the road surface, the well-known Pacejka friction model is used to describe the tire-road friction relationship. The friction equation has proven to properly conform to experimental data with regard to some angular and linear velocity conditions [33]. This friction equation is comprehensive and serves as one of the main employed in vehicle simulators in the market, such as BikeSim, CarSim, and Adams/Tyre [34]. It is defined by:

$$\mu_x = a\left(1 - e^{-b\lambda} - c\lambda\right) \tag{8}$$

where the parameters a, b, and c are constants of the model and λ is the wheel slip. These constants are respectively defined for various road conditions in Table 1. Figure 3 is the block diagram description of the Pacejka friction equation.

Table 1. Definition of the constants in Pacejka friction equation [34]

Condition of road surface	a	b	c
Dry asphalt	1.28	23.99	0.52
Wet asphalt	0.86	33.82	0.35
Cobblestone	1.37	6.46	0.67
Snow	0.19	94.13	0.06

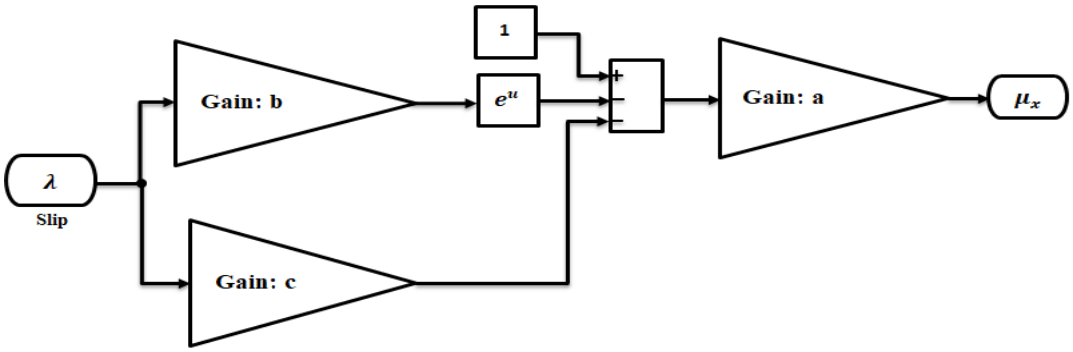

Figure 3. Block diagram of Pacejka friction equation

For a vehicle, the wheel slip equation is represented as follows:

$$\lambda = \frac{v - r\omega}{v} \tag{9}$$

Braking torque T_b, which is the input is not directly linked to λ (the output), as shown in Equation (9). However, the application of the first principle of differentiation to Equation (9), see details in [1], gives:

$$\dot{\lambda} = -\frac{1}{v}\left(\frac{\omega}{mv} + \frac{r^2}{J}\right)\mu(\lambda)N_R + \frac{r}{Jv}T_b \tag{10}$$

where T_b is the control input and is equal to the controller's control action. Figure 4 and Table 2 present the Simulink model of the quarter car dynamic and the description of the parameters. The Simulink model incorporates the air drag force $\frac{1}{2}ADCv^2$ and the wheel's viscous friction f_w.

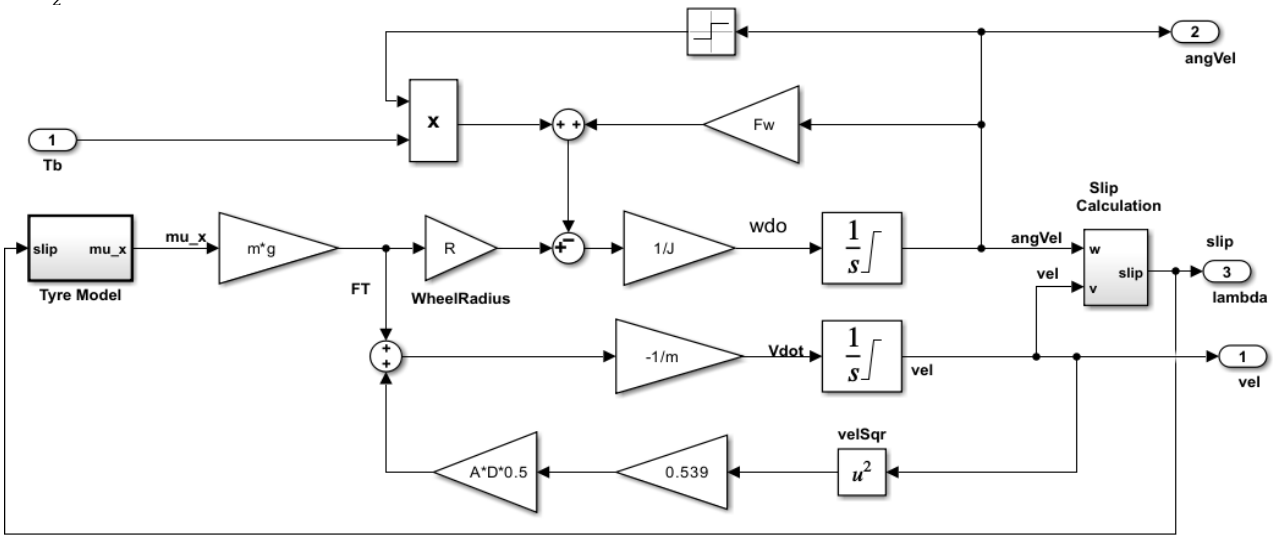

Figure 4. Simulink model of a quarter-car

Table 2. Definition of quarter car parameters [9,32,35]

Definition	Representation	Assigned value
Mass of the quarter car	m	447.5 kg
Wheel radius	r	0.308 m
Moment of inertia	J	1.7kg.m^2
Wheel viscous coefficient	f_w	0.08 Nms.rad^{-1}
Hydraulic time constant	τ	0.0143 s
Acceleration due to gravity	g	9.81 ms^{-2}
Reference slip	λ_r	10%
Pole of actuator	P	70
Gain of hydraulic actuator	k	1.0
Speed of vehicle at initial stage	v_o	30 ms^{-1}
Projected area	A	2.04 m^2
Air density	D	1.225 kgm^{-3}
Drag coefficient	C	0.539

3.2 Wheel Slip Equilibrium Point Analysis

In this subsection, the transient behavior and condition for the equilibrium point regarding slip dynamics are presented. The control design strategy for ABS is centered on maintaining the wheel slip λ as closed as possible to a desired slip λ_r. In [36], a linear transformation of the slip dynamic was performed with respect to the transient behavior and equilibrium condition. The non-linear friction curve was linearized around its optimum value, which is the equilibrium or operating point of wheel slip in ABS. An approximate friction coefficient: $\mu = m_i\lambda$, was achieved from the linearization. Where m_i is the friction curve gradient at the desired operating point [37]. The dynamics of the linearized slip is given by [36]:

$$\dot{\lambda} = -\frac{r^2}{Jv}\mu(\lambda)N_R + \frac{r}{Jv}T_b \tag{11}$$

Taking the Laplace transform of Equation (11) and assuming zero initial condition gives:

$$G_p(s) = \frac{\lambda(s)}{T_b(s)} = \frac{\frac{r}{Jv}}{s + \frac{r^2}{Jv}N_R m_i} \tag{12}$$

Thus, from Equation (12), a pole exists and it is given by:

$$s = -\frac{r^2}{Jv}N_R m_i \tag{13}$$

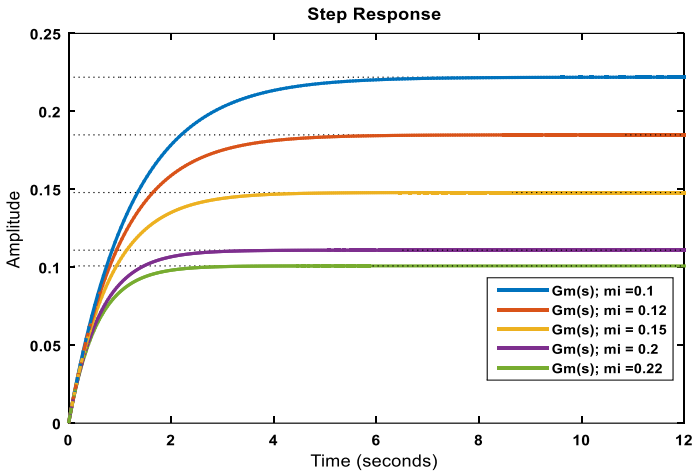

Figure 5. Simulated wheel slip equilibrium point at with varying $\boldsymbol{m_i}$

From Equation (13), it can be seen that system stability within the equilibrium point depends on the gradient of the friction curve m_i. Therefore, the following analysis holds around the operating point. Considering linear approximation, if $m_i < 0$, pole lies on the right-hand side (RHS) of the s-plane, which indicates instability. On the other hand, for $m_i > 0$, the pole lies on the left-hand side (LHS) of the s-plane and this indicates stability [36].

It should be noted that the expression in Equation (12) is a first-order system, which has also been established for a single-tire model for ABS in aircraft braking control [38]. Therefore, considering the fact that the approximated first-order model of the wheel slip can be conveniently used to describe the operating point of wheel slip and define system stability and reference slip tracking, this paper evaluates the effectiveness of this model for a given value of optimal wheel slip performance of 10% by varying m_i as shown in Figure 5. The step response plots in Figure 5 were obtained considering the linearized wheel slip first-order model around the equilibrium point in Equation (12). Substituting the values of the vehicle parameters in Table 2, the values of m_i was varied from 0.1 to 0.22 to give the following expressions:

$$G_p(s) = \begin{cases} G_1(s) = \frac{0.1812}{s + 0.8166}, & m_i = 0.10 \\ G_2(s) = \frac{0.1812}{s + 0.9799}, & m_i = 0.12 \\ G_3(s) = \frac{0.1812}{s + 1.225}, & m_i = 0.15 \\ G_4(s) = \frac{0.1812}{s + 1.633}, & m_i = 0.20 \\ G_5(s) = \frac{0.1812}{s + 1.796}, & m_i = 0.22 \end{cases} \tag{14}$$

Since the objective is to design a controller that will achieve an optimal wheel slip of 10% (or 0.1), at $m_i = 0.22$, this was achieved and the corresponding first order transfer function $G_5(s)$ was taken as the reference model for the ABS.

3.3 Adaptation Mechanism

Given an actual slip λ and a reference wheel slip model λ_m, the difference between them is defined as the tracking error e given by:

$$e = \lambda - \lambda_m \tag{15}$$

The cost function is defined by:

$$J(\theta) = \frac{1}{2}(\lambda - \lambda_m)^2 = \frac{1}{2}e^2 \tag{16}$$

where $J(\theta)$ is the cost function. The cost function can be minimized such that the rate of change in θ is maintained in the direction of the negative gradient of J [39,40] and this is mathematically defined by:

$$\dot{\theta} = -\gamma \frac{\partial J}{\partial \theta} = -\gamma e \frac{\partial e}{\partial \theta} \tag{17}$$

The expression established in Equation (17) is the rate of change in θ so as to minimize the cost function $J(\theta)$ to zero. In addition, $\partial e/\partial \theta$ is called the sensitivity derivative, γ is a positive value that represents a gain of the adaptation mechanism.

Assuming the ABS is a linear process with transfer function $\varphi G(s)$, where φ is an unknown parameter, then the reference model $G_5(s)$ replaced with $G_m(s)$ is defined by:

$$G_m(s) = \varphi_o G(s) \tag{18}$$

where φ_o is a known scalar multiplication of $G(s)$, which is taken as the plant model. Thus, the error given in Equation (15) can be rewritten as a transfer function in s-domain by:

$$E(s) = \varphi G(s)U(s) - \varphi_o G(s)U_c(s) \tag{19}$$

where $\varphi G(s)U(s) = \lambda(\text{s})$, $\varphi_o G(s)U_c(s) = \lambda_m(s)$, and $U(s), U_c(s)$ are the control inputs to the system and the reference model respectively. Thus, the control of the system can be further defined by:

$$U(s) = \theta U_c(s) \tag{20}$$

The substitution of Equation (20) into Equation (19) and taking the partial derivative gives the expression in Equation (21), which is equal to the sensitivity derivative.

$$\frac{\partial E(s)}{\partial \theta} = \varphi G(s)U_c(s) = \frac{\varphi}{\varphi_o}\lambda_m \tag{21}$$

Substituting Equation (21) into Equation (17) gives:

$$\dot{\theta} = -\gamma e \times \frac{\varphi}{\varphi_o}\lambda_m = -y' e \lambda_m \tag{22}$$

or

$$\theta = -\int y' e \lambda_m \, dt \tag{23}$$

where $y' = \gamma \frac{\varphi}{\varphi_o}$ is the update law for θ (adjustment parameter) and stands for the adjustment mechanism of the adaptive controller. The adaptation gain was found to be in the range of $50 \leq \gamma \leq 250$. This range of adaption gain was determined from various simulation trials conducted by substituting different positive values to ascertain the value(s) that provide good control system response performance and reach the setpoint or target wheel slip ratio of 10% (or 0.1) on different road surface conditions. The simulation tests indicated that with selected gains of 50 to 250, the setpoint wheel slip was tracked by the controller with good response performance.

3.4 PID Algorithm

The PID controller combines three algorithms: proportional (P), integral (I) and derivative (D), by leveraging their strengths and weaknesses to achieve optimal control action. The mathematical model of the PID algorithm is defined by:

$$G_{pid}(s) = k_p + \frac{1}{s}k_i + k_d s \tag{24}$$

Equation (24) is an ideal PID controller, which is usually improved by adding a filter to its derivative element. The improved PID is called real PID and it is given by [41]:

$$G_{pid}(s) = k_p + \frac{1}{s}k_i + k_d\left(\frac{N}{1+N/s}\right) \tag{25}$$

where k_p is the proportional gain, k_i is the integral gain, k_d is the derivative gain, and N is the filter coefficient. The PID controller implemented in this work is a discrete-time PID controller like in [1,5,8], which is approximate of the continuous time PID in Equation (25) and it is given by:

$$G_{pid}(s) = k_p + k_i\frac{T_s}{z-1} + k_d\frac{N}{1+NT_s\frac{1}{z-1}} \tag{26}$$

Equation (26) can be simplified as follows:

$$G_{pid}(s) = k_p + k_i\frac{T_s}{z-1} + k_d\frac{N(z-1)}{z-1+NT_s} = 20 + \frac{0.5}{z-1} + \frac{10(z-1)}{z-0.95} \tag{27}$$

where $k_p = 20$, $k_i = 100$, $k_d = 1$, $N = 10$, and sampling time, $T_s = 0.005\ s$. These values were carefully selected after several simulation trials. The reason for the large integral gain compared to the proportional and derivative gains is to ensure that the presence of a steady-state error due to the effect of the increase in wheel slip is swiftly eliminated to reach the setpoint slip by the control system as soon as possible. This is because the control signal will be driven faster to eliminate error by an integral term with a large gain (k_i) than an integral term with a low gain when the steady-state error occurs [42]. The sampling time 0.005 s was basically used to convert the PID controller from continuous time to discrete time and this value has been used in [43,44] for discrete time approximation of event-based fractional order controller and PD controller, respectively.

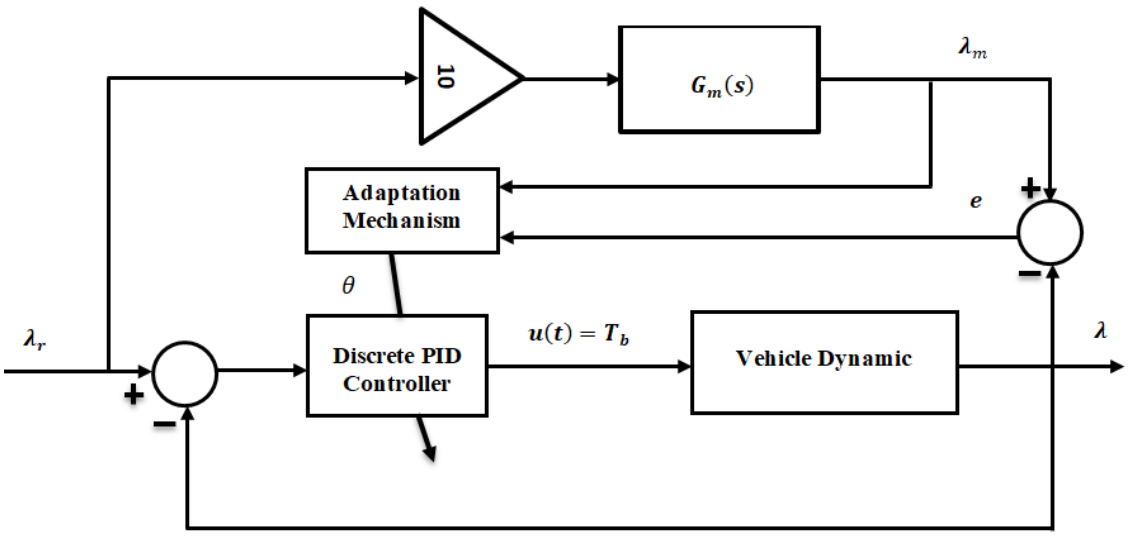

Figure 6. Proposed model of wheel slip control for ABS

The implemented discrete time PID controller is defined in Equation (27). Also, For the purpose of simulation to ensure perfect tracking of the reference or desired wheel slip of 10%, a constant value of 10 was used to multiply the reference slip model, as shown in Figure 6. It should be noted that the majority of road surfaces are considered to have an optimal wheel slip ratio of approximately 0.1 to 0.3 [24]. Also, an essential requirement of the ABS controller is to achieve a wheel slip ratio of 0.08 to 0.18 for dry, wet and icy road surface conditions [18]. Thus, in this work, the control objective

of the proposed controller is to maintain a wheel slip of 0.1 on all road surfaces. In [5], the conventional PID controller in Equation (28), whose parameters where $k_p = 2000$, $k_i = 100000$, $k_d = 1$, $N = 10$, and sampling time, $T_s = 0.005\ s$ was used to achieve slip control and it is used to carry out a comparison with the proposed first-order wheel slip model reference control-based PID controller.

$$G_{pid}(Z) = 2000 + \frac{500}{z-1} + \frac{10(z-1)}{z-0.9} \tag{28}$$

4. SIMULATION RESULTS

The results obtained from simulation analysis conducted in MATLAB/Simulink environment are presented in this section. The system performance analysis was evaluated in terms of varying adaptation gain for different road surface conditions, as shown in Table 1. The parameters considered are the time domain transient characteristics of the wheel in terms of rise time, settling time, peak time, overshoot, and steady-state error. Other response performances are the stopping distance, vehicle braking velocity (speed), and braking torque. The simulation plots obtained when the adaptation gain is 50 are shown in Figures 7(a)-(d). Similarly, for other adaptation gains: 100, 150, 200 and 250, the simulation plots are shown in Figures 8(a)-(d), Figures 9(a)-(d), Figures 10(a)-(d), and Figures 11(a)-(d), respectively. The numerical evaluation of the plots is presented in Tables 3 and 4. Simulation comparison plots and numerical values with previously implemented PID control systems are shown in Figure 12 and Table 5.

The legends are defined as follows: RSM –reference slip model, DRS –dry-asphalt road slip, WRS –wet-asphalt road slip, CSRS –cobblestone road slip, SRS –snow road slip, DRSD –dry-asphalt road stopping distance, WRSD –wet-asphalt road stopping distance, CSRSD –cobblestone road stopping distance, SRSD –snow road stopping distance, DRBV – dry-asphalt road braking velocity, WRBV –wet-asphalt road braking velocity, CSRBV –cobblestone road braking velocity, SRBV –snow road braking velocity, DRBT –dry-asphalt road braking torque, WRBT –wet-asphalt road braking torque, CSRBT –cobblestone road braking torque, and SRBT –snow road braking torque.

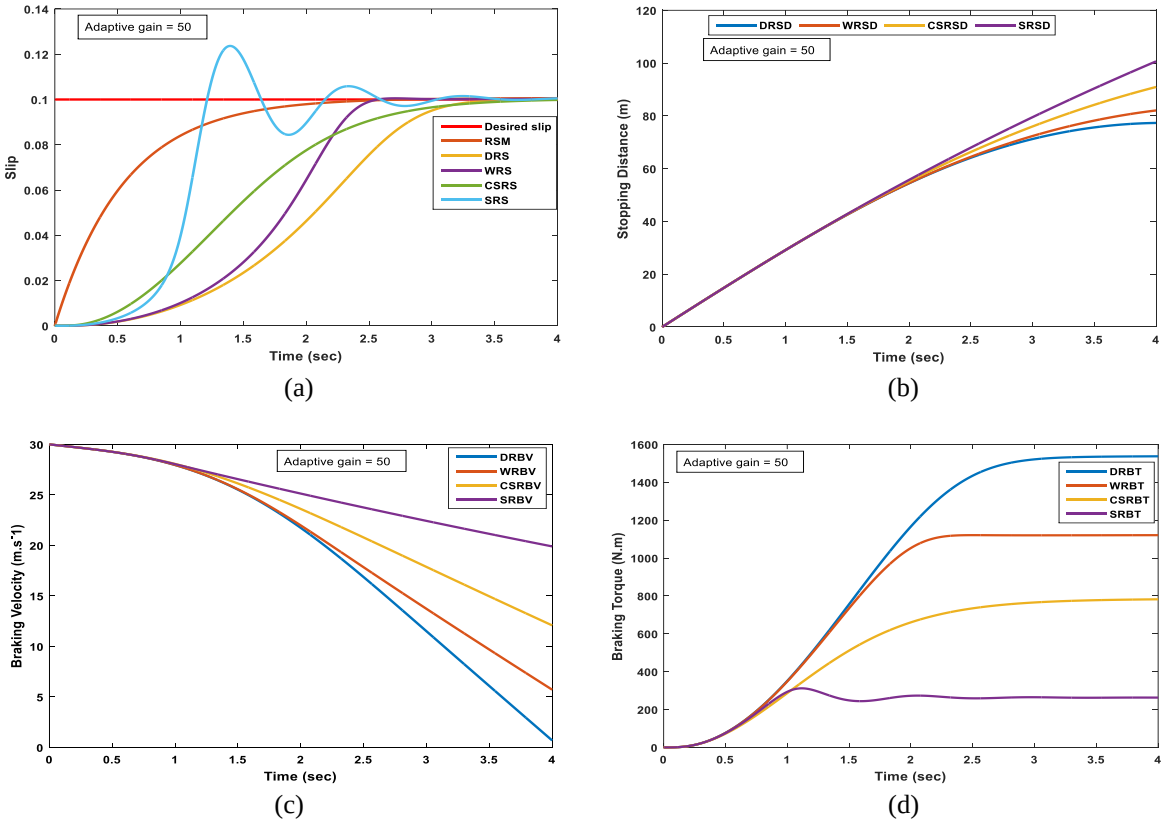

Figure 7. Simulation plots for adaptation gain = 50: (a) wheel slip response, (b) stopping distance, (c) vehicle braking velocity, and (d) braking torque

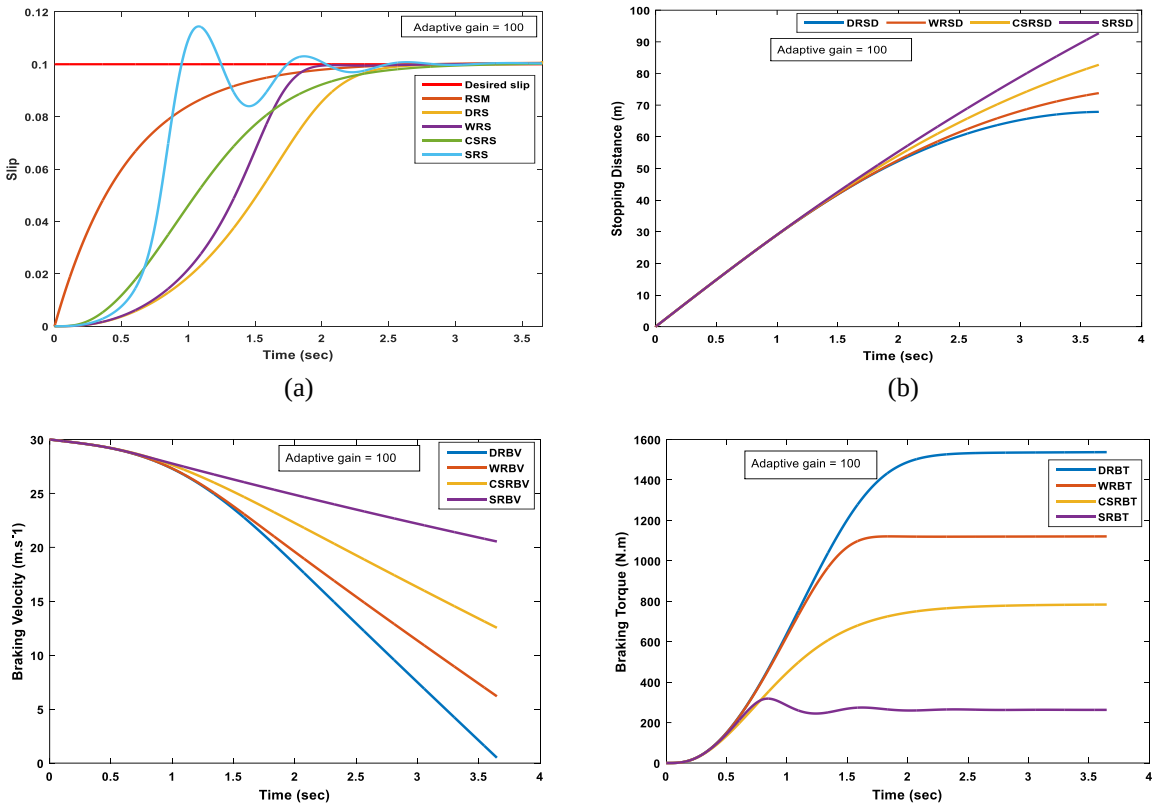

Figure 8. Simulation plots for adaptation gain = 100: (a) wheel slip response, (b) stopping distance, (c) vehicle braking velocity, and (d) braking torque

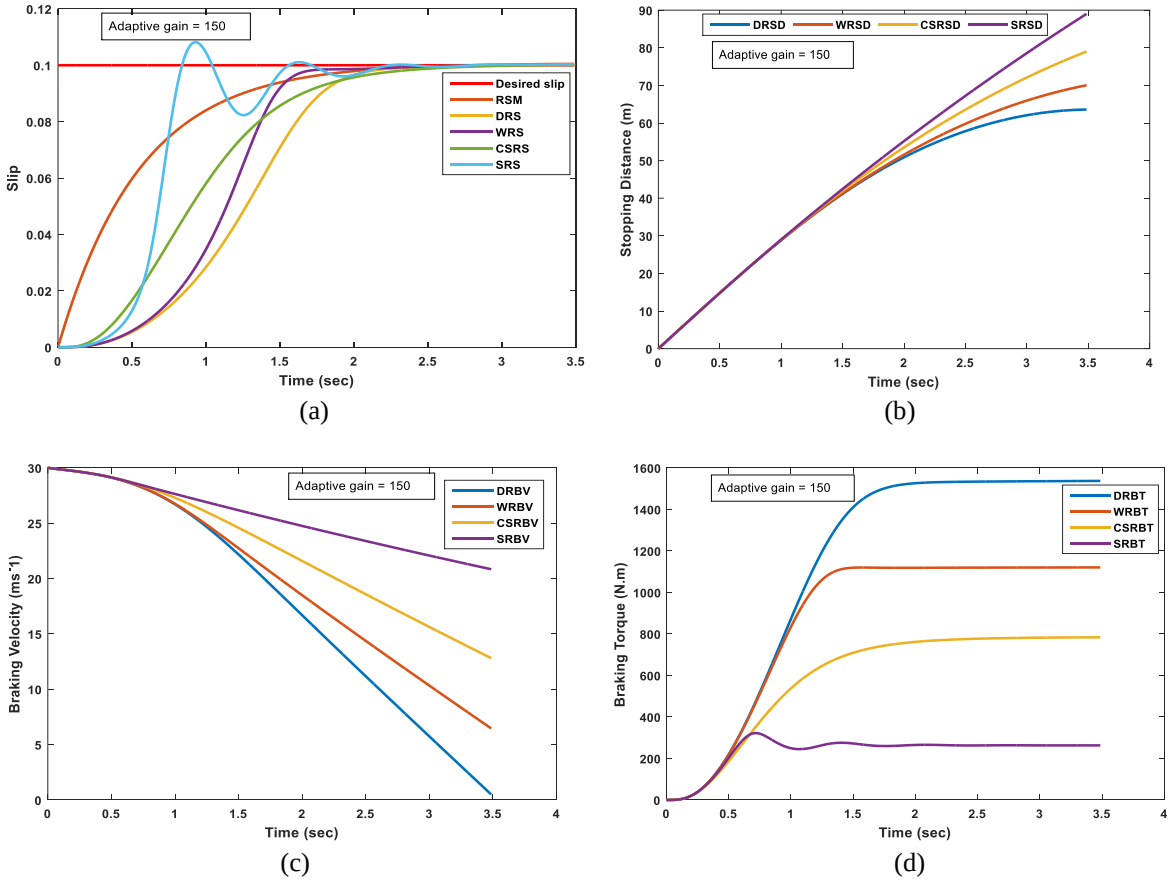

Figure 9. Simulation plots for adaptation gain = 150: (a) wheel slip response, (b) stopping distance, (c) vehicle braking velocity, and (d) braking torque

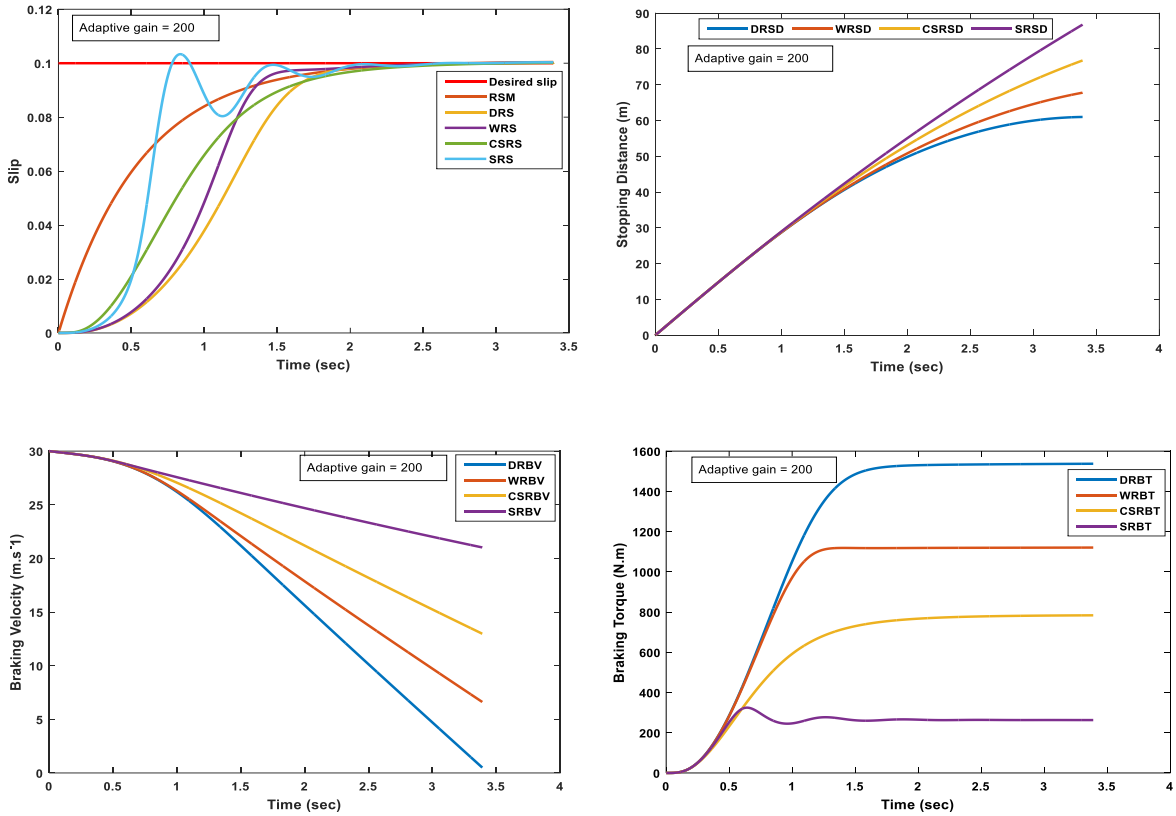

Figure 10. Simulation plots for adaptation gain = 200: (a) wheel slip response, (b) stopping distance, (c) vehicle braking velocity, and (d) braking torque

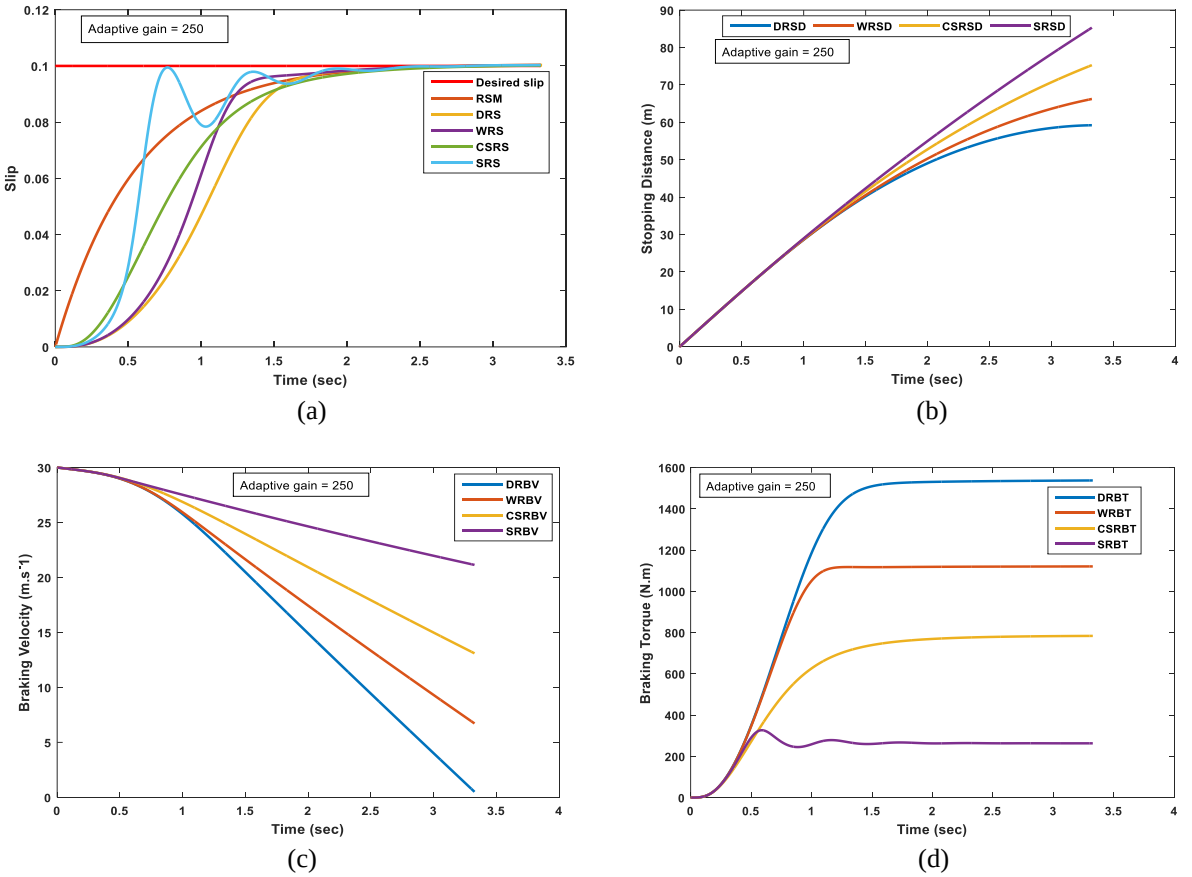

(a) (b)

(c) (d)

Figure 11. Simulation plots for adaptation gain = 250: (a) wheel slip response, (b) stopping distance, (c) vehicle braking velocity, and (d) braking torque

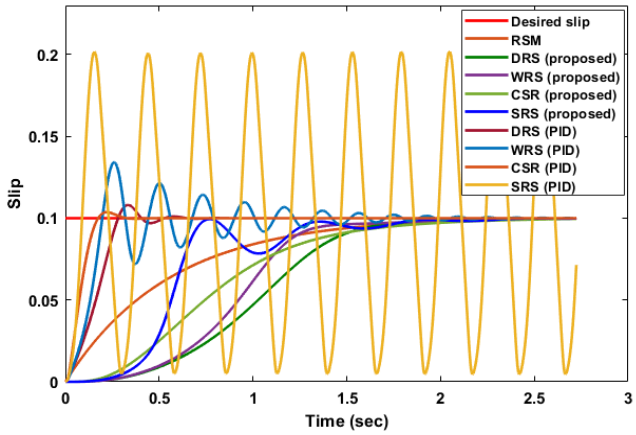

Figure 12. Simulation plots for wheel slip performance comparison of the proposed system and conventional PID

Table 3. Performance of ABS for different adaptation gain

Performance parameter	Dry asphalt	Wet asphalt	Cobblestone	Snow
Adaptation gain $(\gamma) = 50$				
SR	DRS = 0.1	WRS = 0.1	CSRS = 0.1	SRS = 0.1
SD (m)	DRSD = 77.3	WRSD = 82.06	CSRSD = 90.83	SRSD = 100.5
BV (ms^{-1})	DRBV = 0.68	WRBV = 5.71	CSRBV = 12.08	SRBV = 19.9
BT (Nm)	DRBT = 1537	WRBT = 1121	CSRBT = 782	SRBT = 263
Adaptation gain $(\gamma) = 100$				
SR	DRS = 0.1	WRS = 0.1	CSRS = 0.1	SRS = 0.1
SD (m)	DRSD = 67.88	WRSD = 73.76	CSRSD = 82.75	SRSD = 92.67
BV (ms^{-1})	DRBV = 0.58	WRBV = 6.19	CSRBV = 12.55	SRBV = 20.54
BT (Nm)	DRBT = 1537	WRBT = 1121	CSRBT = 783.6	SRBT = 263
Adaptation gain $(\gamma) = 150$				
SR	DRS = 0.1	WRS = 0.1	CSRS = 0.1	SRS = 0.1
SD (m)	DRSD = 63.57	WRSD = 70.04	CSRSD = 78.94	SRSD = 89.02
BV (ms^{-1})	DRBV = 0.5	WRBV = 6.46	CSRBV = 12.81	SRBV = 20.84
BT (Nm)	DRBT = 1537	WRBT = 1121	CSRBT = 783.8	SRBT = 263
Adaptation gain $(\gamma) = 200$				
SR	DRS = 0.1	WRS = 0.1	CSRS = 0.1	SRS = 0.1
SD (m)	DRSD = 60.99	WRSD = 67.78	CSRSD = 76.72	SRSD = 86.81
BV (ms^{-1})	DRBV = 0.5	WRBV = 6.62	CSRBV = 13.01	SRBV = 21.02
BT (Nm)	DRBT = 1537	WRBT = 1121	CSRBT = 783.7	SRBT = 263
Adaptation gain $(\gamma) = 250$				
SR	DRS = 0.1	WRS = 0.1	CSRS = 0.1	SRS = 0.1
SD (m)	DRSD = 59.22	WRSD = 66.24	CSRSD = 75.29	SRSD = 85.31
BV (ms^{-1})	DRBV = 0.562	WRBV = 6.72	CSRBV = 13.1	SRBV = 21.14
BT (Nm)	DRBT = 1537	WRBT = 1121	CSRBT = 783.7	SRBT = 263

Note: BT (braking torque), BV (braking velocity), SR (slip ratio), SD (stopping distance),

Table 4. Time domain performance parameters of ABS response for different adaptation gain

Performance characteristics	Dry asphalt	Wet asphalt	Cobblestone	Snow
Adaptation gain $(\gamma) = 50$				
Rise time (s)	1.778	1.295	1.845	0.451
Settling time (s)	3.215	2.465	3.210	2.939
Peak time (s)	4.000	2.705	4.000	1.395
Overshoot (%)	0.000	0.275	0.000	23.032
Steady-state error	0.000	0.000	0.000	0.000

Table 4. (cont.)

Performance characteristics	Dry asphalt	Wet asphalt	Cobblestone	Snow
Adaptation gain (γ) = 100				
Rise time (s)	1.346	0.895	1.432	0.337
Settling time (s)	2.577	1.895	2.601	2.380
Peak time (s)	3.647	4.000	4.000	1.080
Overshoot (%)	0.000	0.000	0.000	13.96
Steady-state error	0.000	0.000	0.000	0.000
Adaptation gain (γ) = 150				
Rise time (s)	1.144	0.854	1.257	0.332
Settling time (s)	2.189	1.717	2.340	2.115
Peak time (s)	3.486	3.486	3.486	0.930
Overshoot (%)	0.000	0.000	0.000	7.777
Steady-state error	0.000	0.000	0.000	0.000
Adaptation gain (γ) = 200				
Rise time (s)	1.029	0.783	1.167	0.312
Settling time (s)	1.995	1.946	2.234	1.950
Peak time (s)	3.375	3.390	3.390	0.835
Overshoot (%)	0.042	0.000	0.000	3.002
Steady-state error	0.000	0.000	0.000	0.000
Adaptation gain (γ) = 250				
Rise time (s)	0.974	0.739	1.115	0.300
Settling time (s)	2.164	1.963	2.181	1.834
Peak time (s)	3.325	3.326	3.326	3.326
Overshoot (%)	0.000	0.000	0.000	0.000
Steady-state error	0.000	0.000	0.000	0.000

Table 5. Time domain performance comparison of the proposed system and conventional PID control system

Performance characteristics	Dry asphalt	Wet asphalt	Cobblestone	Snow
AFOWS-MRAC-PID controller (γ = 250)				
Rise time (s)	0.955	0.735	1.095	0.298
Settling time (s)	1.892	1.880	2.070	1.807
Peak time (s)	2.724	2.724	2.724	2.510
Overshoot (%)	0.000	0.000	0.000	0.039
Steady-state error	0.000	0.000	0.000	0.000
PID controller				
Rise time (s)	0.208	0.142	0.114	0.047
Settling time (s)	0.492	1.762	0.270	2.723
Peak time (s)	0.335	0.220	0.220	2.550
Overshoot (%)	7.870	34.351	3.676	183.773
Steady-state error	0.000	0.000	0.000	0.030

The simulation results shown in Figures 7 to 11 for wheel slip ratios, stopping distances, vehicle braking velocity, and braking torques with the proposed AFOWS-MRAC-PID controller revealed its ability to track the desired wheel slip and achieve 10% (or 0.1) slip ratio for the range of adaptation gains under simulation time of 4 s. The summary of the numerical analyses obtained from the plots shown in Table 3 indicates that for braking on road surfaces (dry, wet, cobblestone, and snow), all the adaptation gains yielded a 10% slip. With adaptation gains 50, 100, 150, 200, and 250 implemented for dry asphalt, the stopping distances are: (77.3 m, 67.88 m, 63.57 m, 60.99 m, and 59.22 m), the vehicle braking velocities are: (0.68 ms^{-1}, 0.578 ms^{-1}, 0.5 ms^{-1}, 0.5 ms^{-1}, and 0.56 ms^{-1}), and the braking torque remains the same as 1537 Nm in all cases. With braking on wet asphalt for the different adaptation gains 50, 100, 150, 200, and 250, the stopping distances are: (82.06 m, 73.76 m, 70.04 m, 67.78, and 66.24 m), the vehicle braking velocities are: (5.711 ms^{-1}, 6.19 ms^{-1}, 6.46 ms^{-1}, 6.62 ms^{-1}, and 6.72 ms^{-1}), and the braking torque remains 1121 Nm in all cases. On cobblestone, for

different adaptation gains 50, 100, 150, 200, and 250, the stopping distances are: (90.83 m, 82.75 m, 78.94 m, 76.72 m, and 75.29 m), the vehicle braking velocities are: (12.08 ms^{-1}, 12.55 ms^{-1}, 12.81 ms^{-1}, 13.01 ms^{-1}, and 13.1 ms^{-1}), and the braking torque in all cases is 783.7 N.m. Considering braking on snow road surface, for 50, 100, 150, 200, and 250 adaptation gains, the stopping distances are: (100.5 m, 92.67 m, 89.02 m, 86.81 m, and 85.31 m), the vehicle braking velocities are: (19.9 ms^{-1}, 20.54 ms^{-1}, 20.84 ms^{-1}, 21.02 ms^{-1}, and 21.14 ms^{-1}), and the braking torque is 263 Nm in all cases. From the numerical analyses, a 10% wheel slip ratio was achieved by the controller during braking on all road surface conditions considered. Nevertheless, the performance parameters, such as stopping distances, vehicle braking velocities, and braking torques, were different with respect to road surfaces. With respect to stopping distances, vehicle braking velocities, and braking torques for the different adaptation gains, the finest performance was achieved on dry road surfaces, while the least was recorded on snow road surfaces. In Table 4, the time domain response performances revealed that the best results in terms of rise time, settling time and peak time at reduced overshoot were achieved for an adaptation gain of 250.

In Figure 12 and Table 5, the wheel slip responses of the proposed controller on different road surfaces with an adaptation gain of 250 were compared with that of the conventional PID controller from previous studies under a simulation time of 3 s. The adaptation gain 250 was used for the comparison because it is the value that yielded the best performance amongst other adaptation gains. Thus, looking at Figure 12, it can be seen that the PID controller suffers from high oscillation in wet and snow road surfaces. The numerical analysis in Table 5 shows that the PID controller yielded better rise time and settling time on road surfaces than the proposed controller, but on snow road surfaces, it achieved a final wheel slip of 0.07, resulting in a steady state error of 0.03. Furthermore, the PID controller shows good performance on dry and cobblestone road surfaces but with the presence of slight oscillation (or instability) during emergency braking. The proposed controller achieved the desired wheel slip on all road surfaces and showed no oscillation during emergency braking in all cases using an adaptation gain of 250. Hence, with this ability to provide robust control by tracking the desired wheel slip for all road surfaces with no oscillation, the proposed controller outperformed the conventional PID control system.

Generally, the proposed AFOWS-MRAC-PID controller yielded an optimal wheel slip of 0.1 on all road surfaces with respect to the different adaptation gains. The controller utilized the highest braking torque of 1537 Nm on dry road surfaces, while the least (263 Nm) was used on snow road surfaces. This can be said to be the reason for achieving the best stopping distance and vehicle braking (or stopping) velocity on dry road surfaces and the least on snow road surfaces. However, while the controller achieved good transient response performance on all road surfaces, in the case of snow road surface, the ABS experienced high oscillation in terms of overshoot (23.032% and 13.96%) for adaptation gains of 50 and 100. With adaptation gains of 150, 200 and 250, the overshoot for the oscillation (instability), which initially occurs in the ABS during braking on the snow road surface, was reduced to 7.777%, 3.002% and 0, respectively. Looking at Tables 3 and 4, it can be seen that the controller provided the best performance in terms of stopping distance, vehicle braking velocity, braking torque, rise time, settling time, and overshoot on all road surfaces when adaptation gain was 250.

5. CONCLUSIONS

In this paper, a first attempt has been made to control and achieve optimal wheel slip tracking of 10% in ABS using an MRAC-based PID controller centered on the concept of wheel slip equilibrium point. The technique involves ensuring that the entire nonlinear model of wheel slip in ABS control is conditioned to follow the behavior of the approximated wheel slip model for optimal tracking and good hard braking performance. The controller uses a range of adaptation gains to achieve good wheel slip control performance. It should be noted that the primary aim of the controller is to achieve a 10% slip. However, the overshoot of 23.032% was achieved on the snow road surface when the adaptation gain was 50. This does not in any way cancel the effectiveness of the proposed system since other gains can be implemented in any case within the defined range to replace adaptation gain 50. This is one of the reasons for the thorough simulation being carried out to establish a good range of gains for the system's effectiveness. Compared with the performance of the conventional PID controller given in Equation (28), which has been implemented in [5], AFOWS-MRAC-PID yielded better transient response performance and stability in terms of overshoot, especially on wet and snow road surfaces. Future studies intend to incorporate intelligent algorithms into the control loop to ensure that the associated high overshoots using some of the adaptation gains are eliminated. Alternatively, further investigation can be carried out by further tuning the PID controller or by simply implementing the adaptation gains 150, 200, and 250 only to adjust the PID controller. Authors are currently working on substituting the classical PID controller with an intelligent tuned algorithm such as a fuzzy logic controller for the Approximate First Order Wheel Slip Model Reference Adaptive Control.

ACKNOWLEDGEMENT

The authors very much appreciate the management of the Imo State University (IMSU) and the Federal University of Technology Owerri (FUTO) for the enabling environments under which this study was carried out.

REFERENCES

[1] P.C. Eze, F.A. Aigbodioh, C. Muoghalu, and I.H. Ezeanya, "Linear slip control for improved antilock braking," *International Research Journal of Advance Engineering and Science*, vol. 3, no. 1, pp. 198-206, 2018.

[2] G.F. Mauer, "A fuzzy logic controller for an ABS braking system, "*IEEE Transactions on Fuzzy Systems*, vol. 4, no. 4, pp. 381-388, 1995.

[3] W.K. Lennon and K.M. Passino, "Intelligent control for brake systems," *IEEE Transactions on Control Systems Technology*, vol. 7 no. 2, pp. 188-202, 1999.

[4] B.C. Agwah and P.C. Eze, "An intelligent controller augmented with variable zero lag compensation for antilock braking system," *International Journal of Mechanical & Mechatronics Engineering*, vol. 16, no. 11, pp. 303-310, 2022.

[5] P.C. Eze, B.O. Ekengwu, N.C. Asiegbu, and T.I. Ozue, "Adjustable gain enhanced fuzzy logic controller for optimal wheel slip ratio tracking in hard braking control system," *Advances in Electrical and Electronic Engineering*, vol. 19, no. 3, pp. 231-242, 2021.

[6] A.A.Aly, E.S. Zeidan, A. Hamed, and F. Salem, "An antilock-braking system (ABS) control: A technical review," *Intelligent Control and Automation*, vol. 2, pp. 186-195, 2011.

[7] V.R. Aparow, F. Ahmad, K. Hudha and H. Jamaludin, "Modelling and PID control of antilock braking system with wheel slip reduction to improve braking performance," *International Journal of Vehicle Safety*, vol. 6, no. 3, pp. 265–296, 2013.

[8] P.C. Eze and I.E. Achumba, "Investigation of slip minimization in vehicles under different drag coefficients," in *2017 IEEE 3rd International Conference on Electro-Technology for National Development*, pp. 1–9, 2017.

[9] S. John and J.O. Pedro, "Hybrid feedback linearization slip control for anti-lock braking system," *Acta Polytechnica Hungarica*, vol. 10, no. 1, pp. 81–99, 2013.

[10] S.I. Haris, F. Ahmad, M.H. Che Hassan, A.K. Mat Yamin, and N.R. Mat Nuri, "Self tuning PID control of antilock braking system using electronic wedge brake," *International Journal of Automotive and Mechanical Engineering*, vol. 18, no. 4, pp. 9333-9348, 2021.

[11] M. Singh, A. Rani , and V. Singh, "Wheel slip-based intelligent controller design for anti-lock braking system," *Advanced Research in Electrical and Electronic Engineering*, vol. 1, no. 3, pp. 82–88, 2014.

[12] V. Vodovozov, E. Petlenkov, A. Aksjonov, and Z. Raud, "Fuzzy gradient control of electric vehicles at blended braking with volatile driving conditions," in *Proceeding 17th International Conference on Informatics in Control, Automation and Robotics*, pp. 250-261, 2020.

[13] G. Li, T. Wang, R. Zhang, F.Gu, and J. Shen, "An improved optimal slip ratio prediction considering tyre inflation pressure changes," *Journal of Control Science and Engineering*, vol. 2015, no. 1, p. 512024, 2015.

[14] A.B. Sharkawy, "Genetic fuzzy self-tuning PID controllers for antilock braking systems," *Engineering Applications of Artificial Intelligence*, vol. 23, pp. 1041–1052, 2010.

[15] V. Ćirović and D. Aleksendrić, "Adaptive neutron-fuzzy wheel slip control," *Expert Systems with Applications*, vol. 40, pp. 5197–5209, 2013.

[16] S.R. Gampa, K. Jasthi, S. Alapati, S.K. Gudey, and V.E. Balas, "Fuzzy genetic algorithm based antilock braking system," in *Proceedings of the International Conference on Artificial Intelligence Techniques for Electrical Engineering Systems*, pp. 13-22, 2023.

[17] A. Aksjonov, K. Augsburg, and V. Vodovozov, "Design and simulation of robust ABS and ESP fuzzy logic controller on complex braking maneuvers," *Applied Sciences*, vol. 6, no. 12, p. 382, 2016.

[18] A. Shahabi, A.H. Kazemian, S. Farahat, and Sarhaddi, "Wheel slip ratio regulation for investigating the vehicle's dynamic behavior during braking and steering input," *Mechanics & Industry*, vol. 22, p. 17, 2021.

[19] X.-D. Zhang and C.-K. Chen, "A study of a cornering braking control system for a motorcycle," *Applied Sciences*, vol. 12, no. 24, p. 12575, 2022.

[20] E. Kayacan, Y. Oniz, and O. Kaynak, "A grey system modeling approach for sliding mode control of antilock braking system," *IEEE Transactions on Industrial Electronics*, vol. 56, no. 8, pp. 3244–3252, 2009.

[21] A. Marzbanrad, F. Bruzelius, B. Jacobson, and E. Drenth, "Enhanced sliding mode wheel slip controller for heavy goods vehicles," in *Proceedings of the FISITA 2020 World Congres, Prague, 14-18 September 2020*, pp. 1-6, 2020.

[22] S. Latreche and S. Benaggoune, "Robust wheel slip for vehicle antilock braking system with fuzzy sliding mode controller (FSMC)," *Engineering, Technology & Applied Science Research*, vol. 10, no. 5, pp. 6368–6373, 2020.

[23] J. Sun, X. Xue and K.W.E. Cheng, "Fuzzy sliding mode wheel slip ratio control for smart vehicle anti-lock braking system," *Energies*, vol. 12, no. 13, p. 2501, 2019.

[24] S. Rajendran, S.K. Spurgeon, G. Tsampardoukas, and R. Hampson, "Estimation of road frictional force and wheel slip for effective braking system (ABS) control," *International Journal of Robust and Nonlinear Control*, vol. 29, pp. 736-765,

[25] G.V. Dankan, M. Ramesha, S.B. Sridhara, P.G. Naveena, and K.P. Sachin, "Design of antilock braking system based on wheel slip estimation," *Journal of Physics: Conference Series*, vol. 1706, no. 1, p. 012216, 2020.

[26] Y. He, C. Lu, J. Shen and C. Yuan, "Design and analysis of output feedback constraint control for antilock braking system with time-varying slip ratio," *Mathematical Problems in Engineering*, vol. 2019, no. 1, p. 8193134, 2019.

[27] X. Chen, Z. Dai, H. Lin, Y. Qiu, and X. Liang, "Asymetric barrier Lyapunov function-based wheel slip control for antilock braking system," *International Journal of Aerospace Engineering*, vol. 1, p. 917807, 2015.

[28] Y. Song, S. Wu, and Y. Yan, "Development of self-tuning PID controller based on 115 for indoor air quality control," *International Journal of Emerging Technology and Advanced Engineering*, vol. 3, no. 11, pp. 283-290, 2013.

[29] H. Liu, Q. Yu, and Q. Wu, "PID control model based on back propagation neural network optimized by adversarial learning-based grey wolf optimization," *Applied Sciences*, vol.13, 4767, 2023.

[30] J. Guo, X. Jian, and G. Lin, "Performance evaluation of an anti-lock braking system for electric vehicles with a fuzzy sliding mode controller," *Energies*, vol. 7, no. 4, pp. 6459–6476, 2014.

[31] A. Alleyne, "Improved vehicle performance using combined suspension and braking forces," *Vehicle System Dynamics*, vol. 27, no. 4, pp. 235–265, 1997,

[32] C. Jain, R. Abhishek, and D. Abhishek, "Linear control technique for anti-lock braking system," International Journal of Engineering Research and Applications, vol. 4, no. 8, pp. 104-108, 2014.

[33] C. Canudas-de-Wit, P. Tsiotras, E. Velenis, M.Basset, and G. Gissinger, "Dynamic friction models for road/tire longitudinal interaction," *Vehicle System Dynamics*, vol. 39, pp. 189–226, 2003.

[34] S. M. Savaresi and M. Tanelli, "Active braking control systems design for vehicles," 1st ed. London: Springer-Verlag London, 2010.

[35] M. Watany, "Performance of a road vehicle with hydraulic brake systems using slip control strategy," *American Journal of Vehicle Design*, vol. 2, no. 1, pp. 7-18, 2014.

[36] S. John, "Development of nonlinear real-time intelligent controllers for anti-lock braking systems (ABS)," PhD Thesis, University of the Witwatersrand, Johannesburg, 2012.

[37] D. Yoo, "Model based wheel slip control via constrained optimal algorithm," Master's Thesis, RMIT University, Melbourne, Australia, 2006.

[38] A.W. Ndiaye, J.-M. Biannic, M. Cassaro, C. Combier, and J.-B. Lestage, "Advanced aircraft braking control laws design and validation," in *Proceeding 9th European Conference for Aeronautics and Space Sciences*, pp. 1-16, 2021.

[39] P.C. Eze, C.A. Ugoh, C.P. Ezeabasili, B.O. Ekengwu, and L.E. Aghoghovbia, "Servor position control in hard disk drive of a computer using MRAC integrating PID algorithm," *American Journal of Science, Engineering and Technology*, vol. 2, no. 4, pp. 97-105, 2017.

[40] A. Daiifarshchi and S. Bargandan, "Design of a model reference adaptive controller using modified MIT rule for a second order system," *Journal of Artificial Intelligence in Electrical Engineering*, vol. 7, no. 25, pp. 7-14, 2018.

[41] M. Micev, M. Ćalasan, Z.M. Ali, H.M. Hasanien, and S.H.E. Abdel Aleem, "Optimal design of automatic voltage regulation controller using hybrid simulated annealing - Manta ray foraging optimization algorithm," *Ain Shams Engineering Journal*, vol. 12, no. 1, pp. 641-657, 2021.

[42] Zurich Instruments, "Principles of PID controllers," July 2023, https://www.zhinst.com/others/en/resources/principles-of-pid-controllers

[43] I. Birs, I. Nascu, C. Ionescu, and C. Muresan, "Event-based fractional order control," *Journal of Advanced Research*, vol. 25, pp. 191-203, 2020.

[44] S. Folea, R. De Keyser, I.R. Birs, C.I. Muresan, and C. Ionescu, "Discrete-time implementation and experimental validation of a fractional order PD controller for vibration suppression in airplane wings," *Acta Polytechnica Hungarica*, vol. 14, no. 1, pp. 191-206, 2017.